

N76-28174

IBM Selectric II
Prestige Elite 72

11

UPPER-SURFACE-BLOWING JET-WING INTERACTION*

C. Edward Lan
The University of Kansas

SUMMARY

A linear, inviscid, subsonic compressible flow theory is formulated for predicting the aerodynamic characteristics of upper-surface-blowing configurations. The effect of the thick jet is represented by a two-vortex-sheet model in order to account for the Mach number nonuniformity. The wing loading with the jet interaction effects is computed by satisfying boundary conditions on the wing and the jet surfaces. The vortex model is discussed in detail.

INTRODUCTION

In upper-surface-blowing (USB) configurations, the low-pressure-ratio jet from high by-pass ratio turbofan engines blows directly on the wing upper surface. As the jet is relatively thick, being of the order of 10% of the local chord, the conventional thin jet flap theory has been found to be inadequate to predict the high lift (ref. 1). This means that additional lift may come from the interaction between the wing flow and the thick jet which has higher dynamic pressure than the freestream. Of course, the jet entrainment will increase the lift also, mainly through producing the Coanda effect.

In this paper, a theoretical method will be described for predicting the interaction effects due to nonuniformity in Mach numbers and dynamic pressures in the flow field. The inviscid, linear, subsonic compressible flow theory is assumed.

SYMBOLS

C_L total lift coefficient (circulation lift plus jet reaction lift)

* This work was supported by NASA Langley Grant NSG 1139.

ΔC_L difference in lift coefficients with jet on and off
 ΔC_{L_T} jet induced circulation lift coefficient
 C_μ jet momentum coefficient
 c local chord length, m(ft)
 C_j length of trailing jet included in the analysis, m(ft)
 M number of integration points or Mach number
 N number of chordwise integration points
 N_j number of streamwise vortices on the trailing jet
 \vec{n} unit vector normal to jet surface
 R radius of curvature, m(ft)
 s coordinate tangential to the jet surface
 $T = \rho_o / \rho_j$
 t_j jet thickness, m(ft)
 u nondimensional backwash
 V velocity, m/sec (ft/sec)
 x, y, z rectangular coordinates, with x positive downstream, y positive spanwise to the right and z positive upward
 α angle of attack, deg.
 γ nondimensional vortex density
 δ_f flap angle, deg.
 δ_j jet-deflection angle, deg.
 $\mu = V_o / V_j$
 $\mu' = \mu \cos \alpha$
 ρ density, kg/m³ (slugs/ft³)
 ϕ velocity potential, m²/sec(ft²/sec)
 ψ nondimensional additional perturbation velocity potential

Subscripts:

- c chordwise
- j jet flow
- o outer flow
- s spanwise
- w wing
- ∞ freestream

METHOD OF ANALYSIS

Formulation of the Problem

The perturbation flow fields inside and outside the jet are assumed to be governed by the Prandtl-Glauert equations with M_j and M_o , respectively. The solutions of these equations must satisfy the boundary conditions that the jet surface is a stream surface and the static pressure must be continuous across it, in addition to the usual wing tangency condition. In the linear theory, these conditions can be written as (ref.1)

$$\frac{\partial \bar{\phi}_o}{\partial n} - \frac{\partial \bar{\phi}_j}{\partial n} = \frac{-\vec{V}_\infty \cdot \vec{n}(1-\mu')}{\vec{V}_\infty \cdot \vec{i}} \quad (\text{jet stream surface condition}) \quad (1)$$

$$\frac{\partial \bar{\phi}_j}{\partial s} - T(\mu')^2 \frac{\partial \bar{\phi}_o}{\partial s} = 0 \quad (\text{jet static pressure continuity}) \quad (2)$$

$$\frac{\partial \bar{\phi}_o}{\partial z} = \frac{\partial z_c}{\partial x} - \tan \alpha \quad (\text{wing tangency}) \quad (3)$$

where

$$T = \rho_o / \rho_j \quad (4)$$

and $\bar{\phi}_o$ and $\bar{\phi}_j$ are related to the dimensional velocity potentials ϕ_o and ϕ_j as

$$\phi_o = \bar{\phi}_o V_\infty \cos \alpha, \quad \phi_j = \bar{\phi}_j V_j \quad (5)$$

Since the above problem is linear, it can be decomposed into a wing-alone case with potential $\bar{\phi}_w$ and the interaction case with additional potential ψ .

Let

$$\bar{\phi}_o = \bar{\phi}_{wo} (M_o) + \psi_o (M_o) \quad (6)$$

$$\bar{\phi}_j = \bar{\phi}_{wj} (M_j) + \psi_j (M_j) \quad (7)$$

where $\bar{\phi}_{wo}$ and $\bar{\phi}_{wj}$ satisfy the Prandtl-Glauert equations with respective Mach numbers and the following boundary conditions

$$\frac{\partial \bar{\phi}_{wo}(M_o)}{\partial z} = \frac{\partial z_c}{\partial x} - \tan \alpha \quad (8)$$

$$\frac{\partial \bar{\phi}_{wj}(M_j)}{\partial z} = \frac{\partial z_c}{\partial x} - \tan \alpha \quad (9)$$

Substitution of equations (6)-(7) into equations (1)-(3) gives

$$\frac{\partial \psi_o}{\partial n} - \frac{\partial \psi_j}{\partial n} = - \frac{\vec{V}_\infty \cdot \vec{n}(1-\mu')}{\vec{V}_\infty \cdot \vec{i}} + \frac{\partial \bar{\phi}_{wj}}{\partial n}(M_j) - \frac{\partial \bar{\phi}_{wo}}{\partial n}(M_o) \quad (10)$$

$$\frac{\partial \psi_j}{\partial s} - T(\mu')^2 \frac{\partial \psi_o}{\partial s} = - \frac{\partial \bar{\phi}_{wj}}{\partial s} + T(\mu')^2 \frac{\partial \bar{\phi}_{wo}}{\partial s} \quad (11)$$

$$\frac{\partial \psi_o}{\partial z} = 0 \quad (12)$$

The above equations indicate that there are jumps in normal velocities and tangential velocities across the jet surface. If there is no jet (i.e., $\mu'=1$, $M_o = M_j$ and $T = 1$), these equations show that the additional perturbation potentials will be automatically zero.

Vortex Model

In order to satisfy equations (10)-(11) simultaneously, two vortex sheets are introduced on the jet surface. These vortex distributions will induce normal and tangential velocities in the flow field. To evaluate these induced velocities on the boundaries so that boundary conditions, equations (10)-(12), can be satisfied, the induced velocity integrals are reduced to finite sums through the Quasi Vortex-Lattice Method (Quasi VLM) (ref. 2). The resulting discretized vortex arrangement is as shown in fig. 1. Note that the wing vortices directly below the jet surface are arranged so that they coincide with the jet vortices in location. Furthermore, the shaded region represents part of the nacelle. Since the present computer program does not include the nacelle model, special care must be exercised in this region. If vortex representation of the jet starts from the exit, instead of the leading edge, it has been found that the jet would induce a leading-edge type loading in the middle of the wing. Therefore, the vortex distribution must be extended to the wing leading edge, but with freestream conditions assumed in the nacelle region in the computation.

With the vortex arrangement made, the required induced velocities can be computed and substituted into equations (10)-(12) for the solution of unknown vortex strengths. These equations are satisfied only at a discrete number of control points which are chosen according to the "semi-circle method" as described in the Quasi VLM (ref. 2). These calculations are mostly straightforward, except in computing the induced tangential velocities (i.e., backwash) and representing the jet flap effect. These will be discussed below.

Computation of Induced Tangential Velocities

The induced tangential velocities on the jet surface are needed to satisfy equation (11). At any control point, the induced tangential velocity due to the jet vortex distribution in its neighborhood is simply equal to the vortex density at that control point. Since the vortex density at the control point does not appear in the formulation, it is necessary to express it in terms of those at the vortex points through interpolation, such as Lagrangian interpolation. However, the contribution from those vortices not on the same plane with the control point can not be accurately computed in the usual manner as in computing the induced normal velocities. To illustrate, consider the backwash expression in the two-dimensional flow:

$$u(x, z) = \frac{z}{2\pi} \int_0^1 \frac{\gamma(x') dx'}{(x-x')^2 + z^2} \quad (13)$$

As $z \rightarrow 0$, the integrand of equation (13) will have a second-order singularity. The usual method is not accurate in treating such singularity. Therefore, equation (13) should be rewritten as

$$\begin{aligned} u(x, z) &= \frac{z}{2\pi} \int_0^1 \frac{\gamma(x') - \gamma(x)}{(x-x')^2 + z^2} dx' + \frac{\gamma(x)z}{2\pi} \int_0^1 \frac{dx'}{(x-x')^2 + z^2} \\ &\approx \frac{z}{4\pi} \frac{\pi}{N} \sum_{k=1}^N \frac{\gamma(\theta_k) - \gamma(x)}{(x-x_k)^2 + z^2} \sin \theta_k + \frac{z\gamma(x)}{4\pi} \frac{\pi}{M} \sum_{j=1}^M \frac{\sin \theta_j}{(x-x_j)^2 + z^2} \end{aligned} \quad (14a)$$

where

$$\left. \begin{aligned} x_k &= \frac{1}{2} (1 - \cos \theta_k), \quad \theta_k = \frac{2k-1}{2N} \pi \\ x_j &= \frac{1}{2} (1 - \cos \theta_j), \quad \theta_j = \frac{2j-1}{2M} \pi \end{aligned} \right\} \quad (14b)$$

and

$$M = 2^p N \quad (14c)$$

for interdigitation between the control and integration points in the last summation and p is an arbitrary integer greater than 1.

In the implementation of equation (14a) in the present computer program, it is assumed that $M=8N$ if $N>6$ and $M=16N$ if $N \leq 6$. To compute the tangential velocity at a jet control point due to wing vortices, equation (14a) is applied to three wing vortex strips in the immediate neighborhood of the control point. This is indicated in fig. 2. On the other hand, if the control point is on the jet upper surface, the effect due to all vortices on the jet lower surface in the same streamwise section is computed with equation (14a). Similar principle is applicable if the control point is on the lower surface. This is illustrated in fig. 3. The accuracy of equation (14a) has been illustrated in ref. 3.

Incorporation of Jet Flap Effect in Thick Jet Theory

Due to Coanda effect, the USB jet will follow the wing surface and leave the wing trailing edge at an angle relative to the chord to produce the jet flap effect. This is to produce varying but unknown $\vec{V}_\infty \cdot \vec{n}$ in equation (10) along the trailing jet.

Since

$$\frac{\vec{V}_\infty \cdot \vec{n}}{\vec{V}_\infty \cdot \vec{i}} = -\frac{dz}{dx} + \tan \alpha, \quad (15)$$

it is necessary to relate $\frac{dz}{dx}$ to the unknown jet vortex density. As shown in fig. 4, the irrotationality of the jet flow implies that

$$[V_j + V_j \left(\frac{\partial \bar{\phi}_j}{\partial s}\right)_1](R - t_j/2) = [V_j + V_j \left(\frac{\partial \bar{\phi}_j}{\partial s}\right)_2](R + t_j/2)$$

or

$$\frac{t_j}{R} = T(\mu')^2 \left[\left(\frac{\partial \psi_o}{\partial s}\right)_1 - \left(\frac{\partial \psi_o}{\partial s}\right)_2 + \left(\frac{\partial \phi_{wo}}{\partial s}\right)_1 - \left(\frac{\partial \bar{\phi}_{wo}}{\partial s}\right)_2 \right] = f(x,y) \quad (16)$$

$$\frac{1}{R} \approx \frac{d^2 z}{dx^2} \quad (17)$$

where the subscripts 1 and 2 denote the upper and the lower jet surfaces, respectively, at the section under consideration. Equations (16)-(17) give the following initial value problem for determining $\frac{dz}{dx}$:

$$t_j \frac{d^2 z}{dx^2} = f(x,y) \quad (18)$$

$$z(\text{t.e.}) = 0$$

$$\frac{dz}{dx}(\text{t.e.}) = -\delta_j$$

To integrate the above problem for $\frac{dz}{dx}$, a finite jet length C_j is first chosen (It is not necessary to include infinite length of jet in the numerical

method as far as the wing loading is concerned). Then let

$$x = x_{t.e.} + \frac{C_j}{2} (1 - \cos \theta) \quad (19)$$

It follows that

$$t_j \frac{d}{d\theta} \left(\frac{dz}{dx} \right) = \frac{C_j}{2} \sin \theta f(\theta, y)$$

and after integration once,

$$t_j \left(\frac{dz}{dx} \right)_i = -t_j \delta_j + \int_0^{\theta_1} \frac{C_j}{2} \sin \theta f(\theta, y) d\theta$$

$$\approx -t_j \delta_j + (\Delta\theta) \frac{C_j}{2} \left[\sum_{k=1}^{i-1} \sin \theta_k f(\theta_k, y) + \frac{1}{2} \sin \theta_i f(\theta_i, y) \right] \quad (20)$$

by trapezoidal rule. With $\frac{dz}{dx}$ determined by equation (20) in terms of $f(\theta, y)$ and hence, $\frac{\partial \psi_0}{\partial s}$ through equation (16), it is possible to incorporate these terms with unknown vortex densities to the left hand side of equation (10) before equations (10)-(12) are solved.

Note that equations (10)-(12) are solved by the vector method of Purcell (ref. 4) which processes row by row of the augmented matrix in solving the equations. Since the tangential velocities are needed in equation (10) with the jet flap effect (see equation 16), equation (11) must be processed first with the tangential velocities computed there stored on file before equation (10) can be solved.

SOME NUMERICAL RESULTS

Before the method can be applied to any configurations, it is important to know how the discretized vortices should be arranged to produce reliable results. In the following, some convergence study with respect to the vortex arrangement for the configuration used by Phelps, et al. (ref. 5) will be presented. Fig. 5 shows the effects of number of vortices on the trailing jet with $C_j = 1c$ and $2c$. It is seen that 6 vortices ($N_j = 6$) with $C_j = 1c$ appear to be sufficient in applications. If C_j is increased to $2c$, more vortices would be needed to provide convergence. Fig. 6 indicates the rapid convergence of ΔC_{L_T} with respect to the number of wing spanwise vortex strips.

The above method is now applied to the configuration of ref. 5 with 30° full span flap. The jet-deflection angle is taken to be the angle of flap extension relative to the chord line. It is found to be 46.7° . The C_L values were computed by adding predicted ΔC_L to the experimental jet-off C_L . The results are shown in fig. 7. The predicted values are slightly higher possibly because the estimated jet angle was too high. On the other hand, the thin jet flap theory by the present method (ref. 1) would underestimate the lift.

To illustrate the importance of improved tangential velocity evaluation (see equation 14a), the configuration of ref. 6 with $\delta_f = 20^\circ$ and 40° is used in fig. 8. It is seen that without the improved integration technique, the predicted lift would be too high.

CONCLUDING REMARKS

A vortex model for the USB jet-wing interaction has been described. The model consists of using two vortex sheets on the jet surface to account for Mach number nonuniformity and differences in jet and freestream dynamic pressures. The rate of numerical convergence with respect to the number of vortices used appeared to be reasonably rapid. Comparison of the predicted results with some available data showed much better agreement than the thin jet flap theory.

REFERENCES

1. Lan, C. Edward; and Campbell, James F.: Theoretical Aerodynamics of Upper-Surface-Blowing Jet-Wing Interaction. NASA TN D-7936, 1975.
2. Lan, C. Edward: A Quasi Vortex-Lattice Method in Thin Wing Theory. Journal of Aircraft, Vol. 11, No. 9, Sept. 1974, pp. 518-527.
3. Lan, C. Edward: Some Applications of the Quasi Vortex-Lattice Method in Steady and Unsteady Aerodynamics. Vortex-Lattice Utilization, NASA SP-405, 1976. (Paper no. 21 of this compilation.)
4. Purcell, E. W.: The Vector Method of Solving Simultaneous Linear Equations. Journal of Math. and Phys., Vol. 32, July-Oct. 1953, pp. 180-183.
5. Phelps, Arthur E.; Letko, William; and Henderson, Robert L.: Low-Speed Wing-Tunnel Investigation of a Semispan STOL Jet Transport Wing-Body with an Upper-Surface Blown Jet Flap. NASA TN D-7183, 1973.
6. Smith, Charles C., Jr.; Phelps, Arthur E., III; and Copeland, W. Latham: Wind-Tunnel Investigation of a Large-Scale Semispan Model with an Unswept Wing and an Upper-Surface Blown Jet Flap. NASA TN D-7526, 1974.

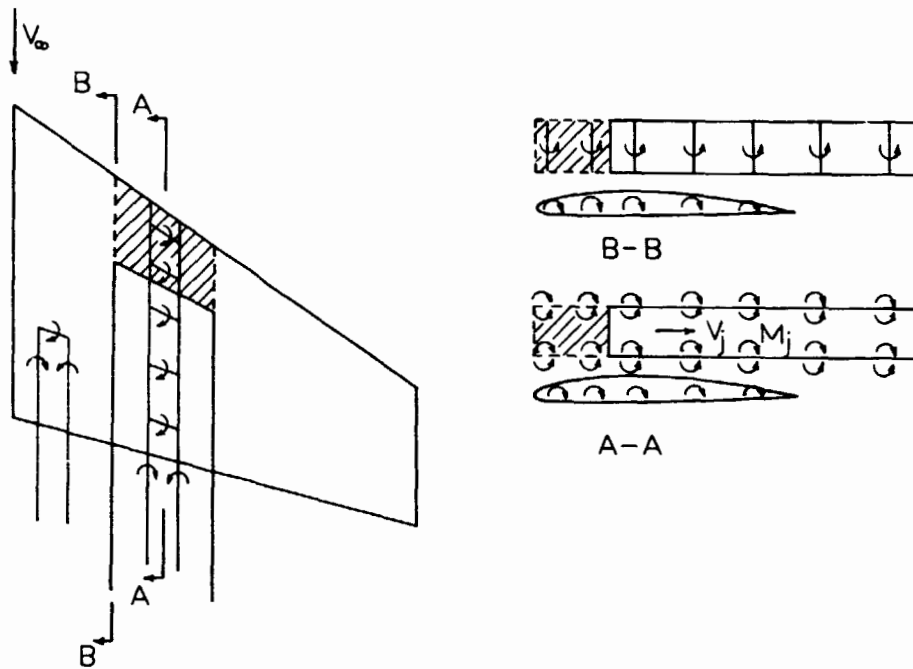


Figure 1.- Vortex model for computing jet-interaction effects.

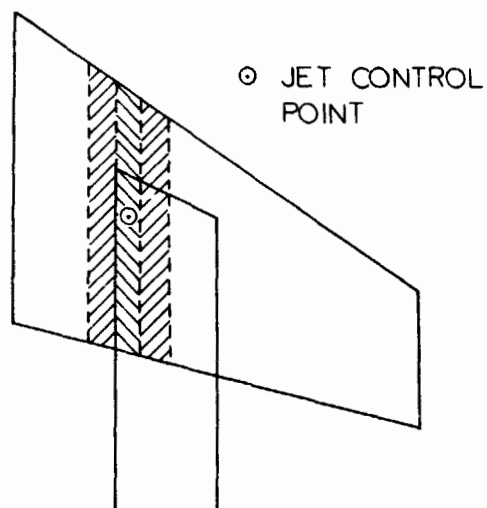


Figure 2.- Region (shaded area) of wing vortex strips subject to improved integration procedure of equation (14a) for computing u -velocity at a jet control point.

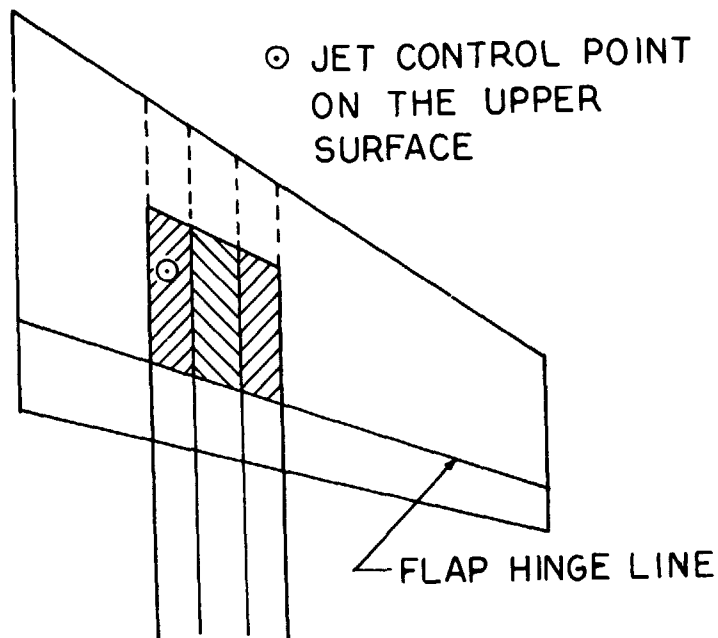


Figure 3.- Region (shaded area) of jet vortex strips on the lower surface subject to improved integration procedure of equation (14a) for computing u-velocity at a jet control point.

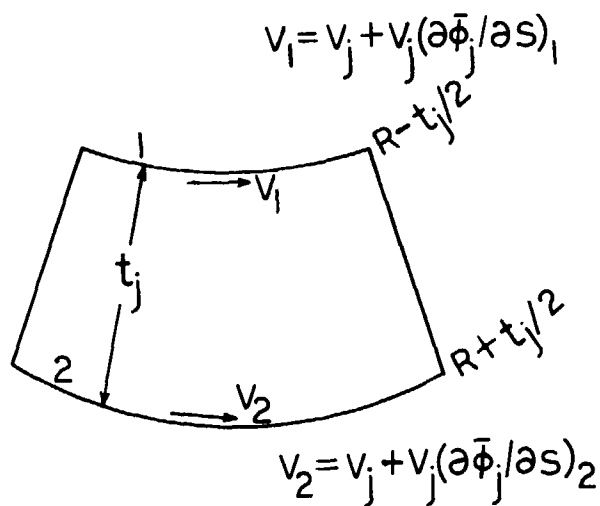


Figure 4.- Geometry of a jet cross section for formulating jet flow irrotationality condition.

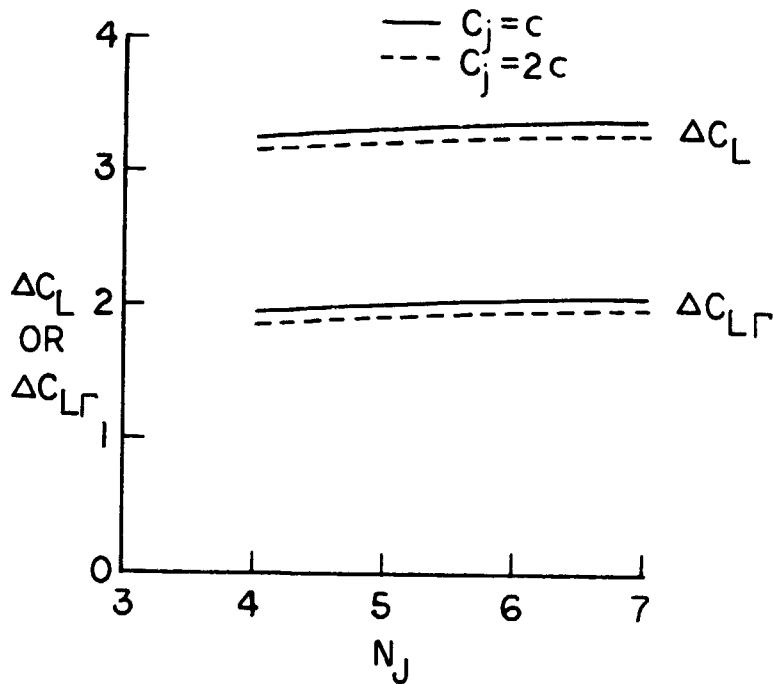


Figure 5.- Effect of number of trailing jet vortices on predicted lift.
 $C_\mu = 0.8 \times 2.095$; $\alpha = 5^\circ$; $\delta_f = 30^\circ$; $\delta_j = 46.7^\circ$; $N_c = 6$; $N_s = 9$.

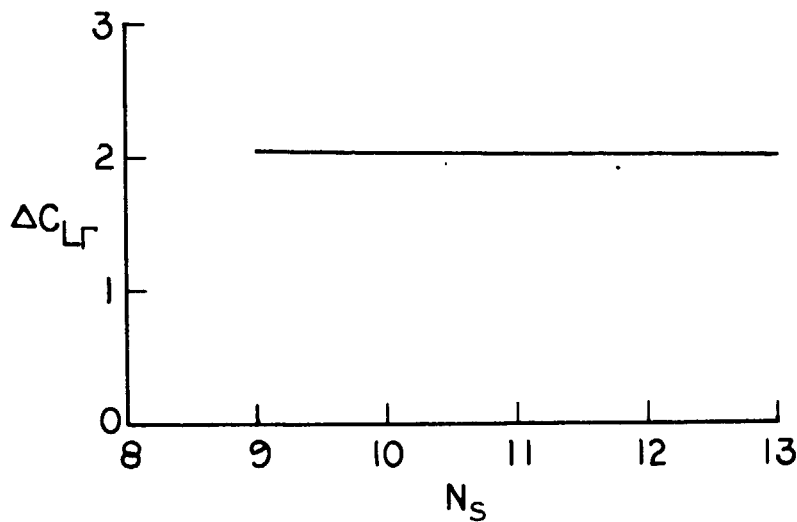


Figure 6.- Effect of number of wing vortex strips on predicted lift.
 $C_\mu = 0.8 \times 2.095$; $\alpha = 5^\circ$; $\delta_f = 30^\circ$; $\delta_j = 46.7^\circ$; $N_J = 6$; $C_j = 1c$.

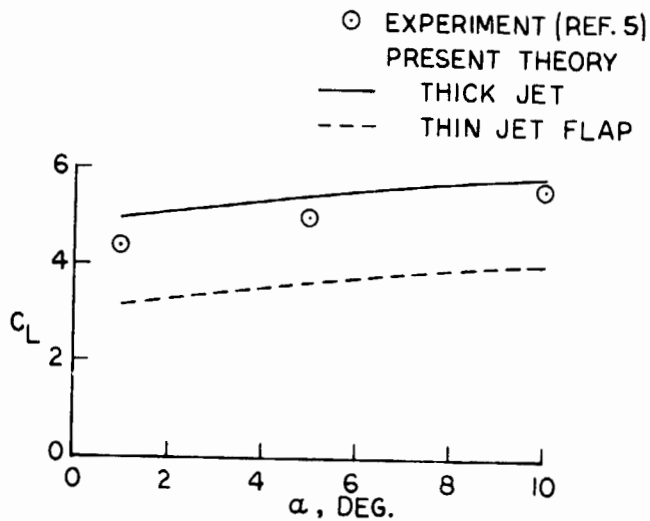


Figure 7.- Comparison of predicted lift curves with experimental data of ref. 4. $C_{\mu} = 0.8 \times 2.095$.

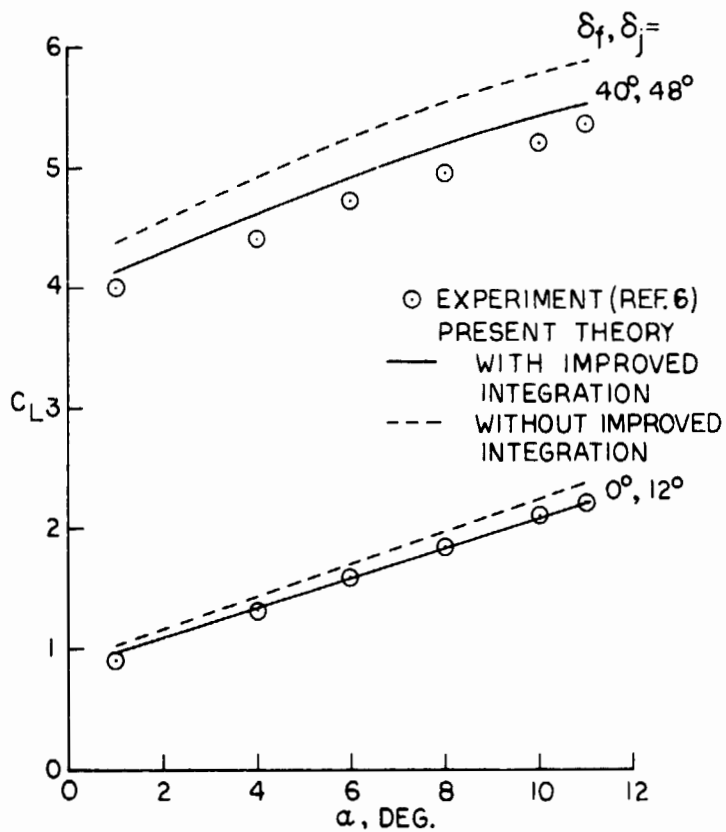


Figure 8.- Effect of backwash evaluation on predicted lift. $C_{\mu} = 2$.